Petrotectonic framework of granitoids and associated granulites at Nagavalli Shear Zone (NSZ), Eastern Ghats Belt: Evidence of a late transpression orogeny

Tamoghna Saha and Subrata Karmakar*

Department of Geological Sciences, Jadavpur University, Kolkata 700 032, India.
Corresponding author. e-mail: subrata.jugeol@gmail.com

Megacrystic granitoids associated with migmatitic and metasedimentary gneisses occurring around Nagavalli Shear Zone (NSZ) preserve complex metamorphic and deformation history. Thinly laminated discontinuous banding of quartzofeldspathic layer (S_1) in the migmatites is the product of first incipient melting during prograde M_1–D_1 tectonothermal event. Peak M_2–D_2 event is manifested by the development of S_2 gneissic foliation in all rocks, which is axial planar to rootless folds on S_1. Porphyroblastic garnet mantled by leucosomal melt fraction in granitoids, suggest that the rock suffered peak granulite facies metamorphism along with host migmatitic gneisses. The subsequent D_3 event deforms differently the massive granitoids and the migmatitic granulite gneisses. The D_4 deformation acted as transpression with broad northwest–southeast compression that develops strong discontinuous regional-scale anastomosing shear zones transecting the earlier gneissosity (S_2) in the granitoids with prominent sinistral shear sense. It deforms the axial plane of regional folds in migmatites and develops superposed non-plane non-cylindrical folds in outcrop to regional scale. Thus we infer megacrystic granitoids were possibly emplaced in pre- to syn-peak metamorphic event within the host granulites. Granitoids and associated migmatitic gneisses of Late Meso- to Neoproterozoic age suffered subsequent petrotectonic events followed by a sinistral transpression acted along NSZ.

1. Introduction

Eastern Ghats Belt (EGB), a deeply eroded high-grade terrane is the product of polycyclic granulite metamorphism (Dasgupta and Sengupta 2003; Mukhopadhyay and Basak 2009; Karmakar *et al.* 2009). Rickers *et al.* (2001) demonstrated Eastern Ghats Belt as collage of juxtaposed terranes. Recently, Dasgupta *et al.* (2013) proposed EGB as accreted crustal fragments, which were amalgamated through discrete orogenic cycles during Paleo–Mesoproterozoic, Meso-Neoproterozoic, and Late Neoproterozoic times (Dobmeier and Simmat 2002; Simmat and Raith 2008; Karmakar *et al.* 2009; Mukhopadhyay and Basak 2009; Bose *et al.* 2011; Das *et al.* 2011). This belt had been classified on the basis of petrographic, lithological, metamorphic, geochronologic as well as structural data (Ramakrishnan *et al.* 1998; Dobmeier and Raith 2003; Chetty 2001). Ramakrishnan *et al.* (1998) introduced a four-fold longitudinal subdivision, viz., Western Charnockite Zone (WCZ), Western Khondalite Zone (WKZ), Central Migmatite Zone (CMZ), and Eastern Khondalite Zone (EKZ). Based on the Nd, Rb–Sr and Pb isotopic signatures of ortho- and paragneissic rocks of the entire EGB,

Rickers *et al.* (2001) subdivided EGB into four crustal domains (figure 1). Domain 1 broadly coincides with western charnockite zone (WCZ) and is subdivided into 1A and 1B. Domain 1A, situated at the southern part, is characterized by homogeneous Nd-model ages for paragneisses (2.8–2.6 Ga) and orhthogneisses (2.5–2.3 Ga). In the northern part, Domain 1B is characterized by older crustal protolith (3.9–3.2 Ga of orthogneisses). Domain 2 consists of central migmatite zone (CMZ) and eastern khondalite zone (EKZ) and shows very complex isotopic characters. Metasediments have Nd model age of 2.5–2.1 Ga, while the orthogneisses have a wide Nd-model age spanning 3.2–1.8 Ga. Domain 3 is situated north of Domain 2 and shows fairly homogeneous Nd-model age (2.2–1.8 Ga for both metasediments and orthogneisses). This domain has more juvenile addition compared to the others. Domain 4 is situated at the extreme northern part with Nd-model age of 3.2 Ga for the orthogneisses and 2.8–2.2 Ga for the metasediments. The essence of the subdivision of EGB is that the protolith

history of all the four crustal domains is contrasting. The sources of the sediments deposited on a basement (of unknown age) are the adjoining Archean cratons, while small but variable quantities of juvenile material was added during Proterozoic age orogenesis. The Nagavalli and Vamasadhara shear zones (NSZ and VSZ) demarcate the Domains 2 and 3 (Chetty 2001). Dobmeier and Raith (2003) on the other hand, subdivided EGB into several metamorphic provinces considering the similarity of petrological and isotopic signatures. The provinces were further subdivided into domains, which are distinguished on the basis of 'lithology, structure and metamorphic grade'. The nature of the mutual boundaries in the domainal or provincial classification is one important aspect. Several workers (Biswal and Sahoo 1998; Chetty 2001; Chetty *et al.* 2003) identified megalineaments in EGB from satellite imagery data although with limited ground checks. These lineaments broadly follow the domain/province boundaries which subdivide the EGB into several structural domains.
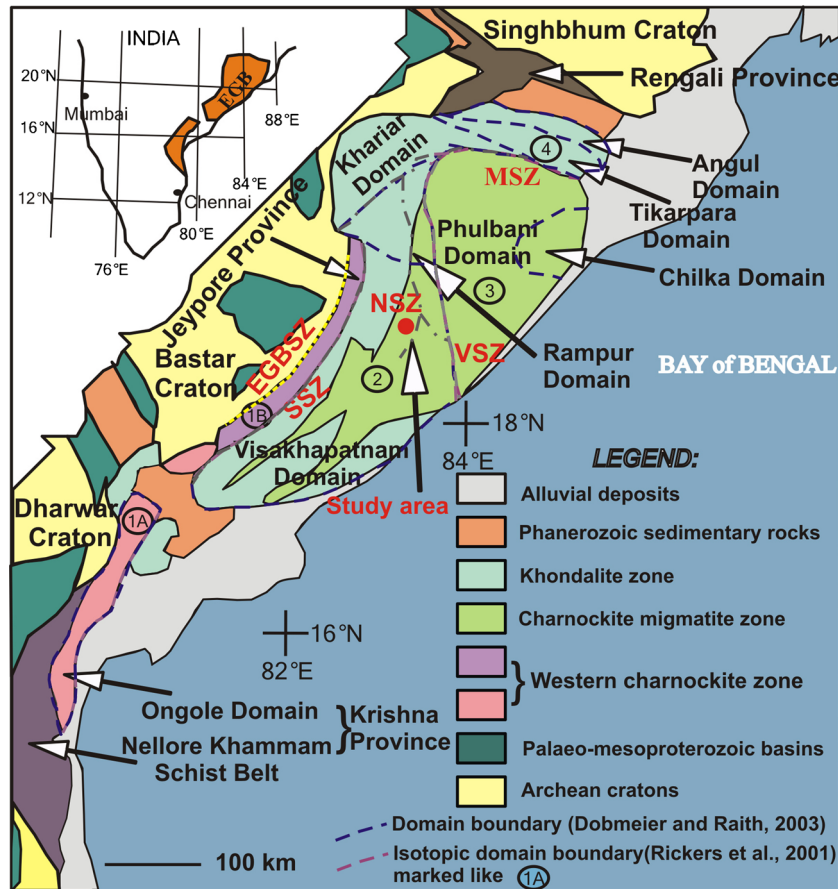

Figure 1. The geological setting of the field area in the Eastern Ghats Belt (EGB), India showing domainal divisions (after Rickers *et al.* 2001) and Province classification (after Dobmeier and Raith 2003) which are transected by major shear zones; Nagavalli Shear Zone (NSZ), Vamasadhara Shear Zone (VSZ), Sileru Shear Zone (SSZ) and Mahanadi Shear Zone (MSZ) after Chetty (2001). Eastern Ghats boundary shear zone is referred as EGBSZ. The nomenclature of Khondalite Zone, Charnockite Migmatite Zone and Western Charnockite Zone are after Ramakrishnan *et al.* (1998). The study area is marked in the figure.

The structural domains signify the low-strain regions bounded by high-strain areas in the form of shear zones as suggested by Chetty (2001) and Chetty *et al.* (2003).

Orogenic shear zones develop as a result of large crustal displacement through a collisional event, which ranges from syn- to post-orogenic periods. The syn-orogenic shear zones are created close to the subduction front whereas, terrane boundary shear zone is created at the juxtaposition of slices of crust towards the overriding plate (Moresi *et al.* 2014). Several workers argue that thrusting of hot granulites along westward direction and welding of Proto Indian crust with EGB occurred during the Grenvillian through docking of hot UHT metamorphosed rocks over the Indian cratonic nucleus of Bastar Craton (Bhadra *et al.* 2004; Das *et al.* 2008). On the contrary, Biswal *et al.* (2007) indicated that regional metamorphism and fold-thrust structures with final juxtaposition of north-western part of EGB against Bastar Craton had taken place between 617 and 517 Ma along the Terrane Bounday Shear Zone (TBSZ). The other type is within terrane shear zone (Plujim *et al.* 1994). The crust moves and thrusts towards orogenic hinterland when the process of subduction ceases at plate margin or rather orogenic front. Depending upon the rate of accretion at the front, there may be an extension or compression (Cawood *et al.* 2009) in the back-arc area. This creates an environment for shear stress generation in the interior of the orogenic chain away from the collisional margin, and thus orogenic movements get accommodated by contractional or extensional shear zone development (Butler and Freeman 1996). As a result, the hinterland areas and orogen interiors are potential for generation of late- to post-orogenic shear zones. The shear zones develop in orogen interior by the stress generated at the subduction or collision front that permeated towards the interior. The orogen interior shear zones study in EGB is relevant to this background. Recently, Dasgupta *et al.* (2013) suggested prolonged accretion-collision history for central EGB that initiated at 1.5 Ga and culminated at ca 0.90 Ga. The charnockite and granite emplacement took place about 0.98–0.96 Ga and later collision and docking of Domain 2 onto the Bastar Craton occurred at about 0.9 Ga. The docking is manifested by generation or rejuvenation of shear zones in the charnockite and granitoid. Gupta (2012) suggested the late orogenic episodes of EGP were confined to province boundaries.

Chetty (2001) and Chetty *et al.* (2003) characterized the lineaments in EGB as ductile shear zones with limited field structural data. The most prominent of these is the Sileru Shear Zone (SSZ) marking the eastern boundary of WCZ (figure 1). The northernmost part of EGB is separated from the rest of the belt by the Mahanadi Shear Zone (MSZ) trending nearly E–W. Another major lineament is the Nagavalli–Vamasadhara Shear Zone (NVSZ) trending NNW–SSE that demarcates the boundary between the Visakhapatnam and Chilka domains of the Eastern Ghats Province (EGP). The lineaments broadly coincide with the river courses of Nagavalli–Vamasadhara. They inferred that the NVSZ is a result of a prolonged period of shear deformation marked by magmatism, migmatization, and development of ductile shear zones from 1450–850 Ma. The shear zones formed are steeply dipping with gently plunging lineations. The development of high-strain zones is accompanied by melting giving rise to leucogneiss in central parts of the shear zone. The shear zones are suggested to be the product of a transpressive movement in dextral nature. However, Mukhopadhyay and Basak (2009) pointed out the misfit of shear sense of the NSZ lineament compared to other tectonic lineaments of EGB and suggested more detailed study in this respect. The granitoids, on the contrary, are referred to be syntectonic with shearing at about 800 Ma (Kovach *et al.* 1997). However, detailed structural, petrological and geochronological data with real tectonic significance of the lineaments are required to test the character of such domain/province boundaries. The interpretation of post-Grenvillian transpression tectonics for Chilka Lake granulites Dobmeier and Simmat (2002) is noteworthy in this context though the local structures have been explained by overall compressional regime without significant transpression (Das *et al.* 2012).

Alkaline plutonic complexes reported along the shear zones are interpreted to be related pull apart basin structures (Gupta *et al.* 2005; Das *et al.* 2008). However, few workers (Gupta *et al.* 2005; Mukhopadhyay and Basak 2009) questioned the timing of emplacement *vis-à-vis* shearing of these alkaline plutons. Biswal *et al.* (2007) correlated the alkaline magmatism with the fold-thrust belt structures when EGB was juxtaposed against the Bastar Craton. Anorthosite emplacement all over the Eastern Ghats Belt are interpreted to be emplaced much earlier than alkaline plutonic complexes (Dobmeier and Simmat 2002; Dobmeier 2006). Megacrystic granitoids are reported from Eastern Ghats province (EGP) at several localities (Mukhopadhyay and Bhattacharya 1997; Narayana *et al.* 1999; Simmat and Raith 2008) including along the NVSZ (Chetty *et al.* 2003). However, the emplacement of the granitoids, their deformation *vis-à-vis* metamorphism in context of the major shear zones are yet to be ascertained by systematic studies.

From the above backdrop, the study area occupies a key location to record the petrological and

structural attributes of Nagavalli Shear Zone (NSZ) (figure 1). The study area falls within the Domain 2 (Rickers *et al.* 2001), in proximity to Domain 3 towards northeast and is transected by the NSZ. The present work envisages the emplacement of granitoids within the host migmatitic gneisses and metasedimentary rocks of EGB and exploring the style, magnitude, and events of polydeformation polymetamorphism and focuses on the status of NSZ through an integrated study of tectonothermal evolution of granitoid gneisses and associated granulites to resolve the ongoing debated issues. This is also essential to investigate along with the status of NSZ in context of petro-tectonic evolution of Eastern Ghats Belt.

2. Petrological characteristics of granitoids and associated granulites

The study area covers in and around Parvatipuram town in Andhra Pradesh, India (figure 2). It is included in the Domain 2 (Rickers *et al.* 2001) or Visakhapatnam domain (Dobmeier and Raith 2003) in the Eastern Ghats Belt. The area

is situated close to the boundary between Domain 2 and Domain 3 which is transected by the Nagavalli Shear Zone (Chetty *et al.* 2003). The area covering almost 450 km² has been mapped in the scale of 1:50,000 (figure 2). The study area exposes megacrystic granitoids, migmatitic gneisses, khondalite, and quartzite. There are principally two different varieties of granitoids: grey coloured and white coloured, based on the appearance in outcrop scale. The central part of this area is invaded by varieties of granitoids whereas the northwestern part is mostly covered by khondalites and quartzites; the eastern part is dominantly covered by migmatitic gneisses. However, khondalite and quartzite also occur in the eastern part and migmatites are associated with other rocks in the northwestern part of the area. Granitoids have sharp and intrusive contacts with charnockite-enderbites and migmatitic gneiss (leptynites) whereas the relation with khondalites is not exposed. The granitoids are macroscopically crudely foliated, to extremely sheared in nature. Both grey- and leuco-granitoids consist of euhedral/rectangular feldspar grains, which on continued deformation
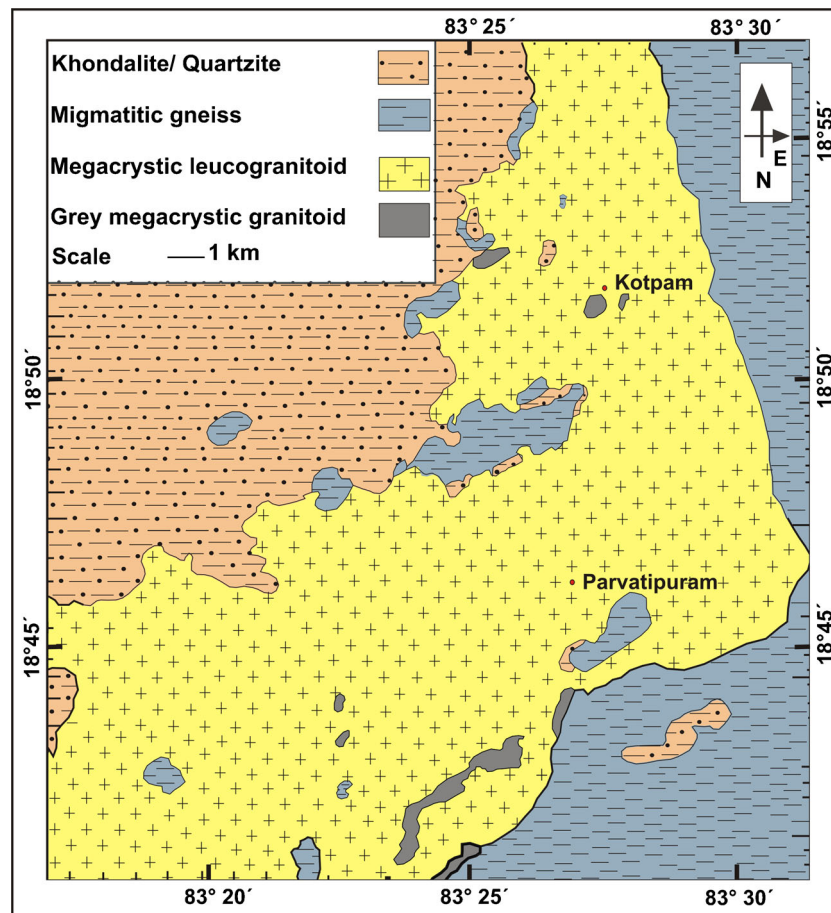

Figure 2. Disposition of rock types in the lithological map of the study area, originally mapped on 1:50,000 scale.

transformed to augen shaped clasts in sheared granitoids and are characterized by alternately banded flattened light coloured feldspar clasts with dark coloured biotite and garnet rich bands. Henceforth the granitoids are referred as granitoid gneiss. The migmatitic gneisses consist of leptynitic gneiss (quartzo-feldspathic gneiss), massive charnockite-enderbites, migmatitic charnockite, and mafic granulites in outcrop scale. The leptynitic gneiss and both types of charnockites varies in thickness from meter to outcrop scale. However, mafic granulites occurr as bands or lenses within the migmatitic gneisses in tens of cm to meter scale in width. Apart from leptynites and charnockites-enderbites, khondalites (garnet-sillimanite-bearing quartzofeldspathic gneiss) and leucocratic variants of charnockite gneiss (orthopyroxene-bearing quartzofeldspathic gneiss) referred as orthopyroxene bearing migmatite also occur in a few exposures of migmatitic gneisses.

The leuco-granitoids are composed of translucent to opaque plagioclase and milky white alkali feldspar megacrysts (figure 3a). Crudely foliated to highly sheared varieties of leuco granitoids occurr in the area. The mineral constituents are plagioclase (18–22%), alkali feldspar (10–15%), quartz (16–20%), garnet (5–15%), orpthopyroxene (0–5%), ilmenite (5–10%), amphibole (0–2%), clinopyroxene (<2%), biotite (12–16%) mostly. The fine grained matrix is composed of smaller alkali feldspar, plagioclase, biotite, opaque phase, and quartz aggregates. There is coarse garnet with meagre pyroxene and amphibole in it. Pyroxene is not the ubiquitous constituent of leucogranitoids. The rock is characterized by variable proportions of quartzofeldspathic leucosomal fractions. The length of feldspar megacrysts range from 4–7 cm in euhedral grains in relatively unsheared variety and may exceed 10 cm in stretched and sheared variety. Large clusters of garnet (2–6 mm) with included opaque phase and biotite are rimmed by leucocratic melt fraction. The leucosomal patches form melt networks containing garnet and opaque phases and are variably elongated along the gneissic fabric depending upon the intensity of shear deformation. Dark coloured homogeneous decimetre-scale oval, drop to angular shaped mafic microgranular enclaves also occur (figure 3b). The enclaves contain orthopyroxene, clinopyroxene, quartz, feldspar, and locally garnet. In the sheared variety, the granitoids are characterized by the presence of mylonitic foliation that wraps around the feldspar augen. The sheared granitoid gneisses are characterized by the melanocratic and leucocratic bands, stretched along the shear foliation. The melanocratic bands are defined by biotite, garnet, orthopyroxene, and amphibole. Porphyroblastic garnets contain

inclusions of quartz ilmenite, biotite, alkali feldspar, and rarely, plagioclase. Biotite and amphibole occur as an interstitial phase between the feldspar and quartz grains. Alkali feldspar-rich granitoids are devoid of pyroxene and contain euhedral biotite in interstitial space resulting in the matrix fraction with smaller quartz, plagioclase, and garnet grains.

Grey megacrystic granitoids also show variable deformation intensity from less deformed to highly sheared in nature. The mineral constituents are plagioclase (15–20%), alkali feldspar (8–12%), quartz (12–15%), garnet (8–20%), orpthopyroxene (5–10%), ilmenite (8–12%), amphibole (2–5%), clinopyroxene (4–6%), biotite (12–16%) mostly. These are composed of greenish to grey feldspar megacrysts of 5–8 cm with melanocratic matrix made up of quartz, feldspar, garnet, pyroxene, quartz, and amphibole with greasy appearance. Henceforth, the grey megacrystic granitoids may also be referred to as megacrystic charnockites as orthopyroxene is the ubiquitous phase in it. Matrix quartz grains are polygonal inequigranular and interlocking with alkali feldspar and plagioclase grains. The plagioclase aggregates contain coarse subhedral amphibole inclusions. Plagioclase megacrysts are of euhedral to subhedral in shape (figure 3c). There are greyish green polymodal quartzofeldspathic aggregates interfingering in the matrix dominated by plagioclase. Coarse garnet and pyroxene grains are often rimmed by leucosomal fractions in matrix. Porphyroblastic garnet grains with inclusions of biotite, quartz, and opaque phase are surrounded by leucosomal melt fraction in 3–4% of outcrop (figure 3d). Subhedral to anhedral plagioclase feldspars occur with recrystallized border in the sheared variety. Biotite flakes along with garnet clusters are stretched and flattened. There are bands and lenses of mafic microgranular enclaves within sharp to diffuse contact occuring within the leucocratic variety. Orthopyroxene-rich fractions contain lesser proportions of plagioclase clasts. Retrograde biotite replaces the ferromagnesian phases and locally amphibole also surrounds pyroxene grains.

Granitoids with gradational contacts between the above-mentioned varieties in outcrop scale have been observed consisting of 40–65% modal of euhedral to subhedral greyish green feldspar megacrysts. The matrix is composed of stretched up smaller feldspar, quartz, garnet, and biotite clasts.

There are broadly two types of leptynitic gneiss depending upon mineral assemblage and their modal proportion. The grey leptynitic gneiss is a mesocratic rock containing biotite, opaque phase, garnet along with quartzofeldspathic phase while the white leptynite consists of leucosomal quartzofeldspathic melt containing insignificant to low
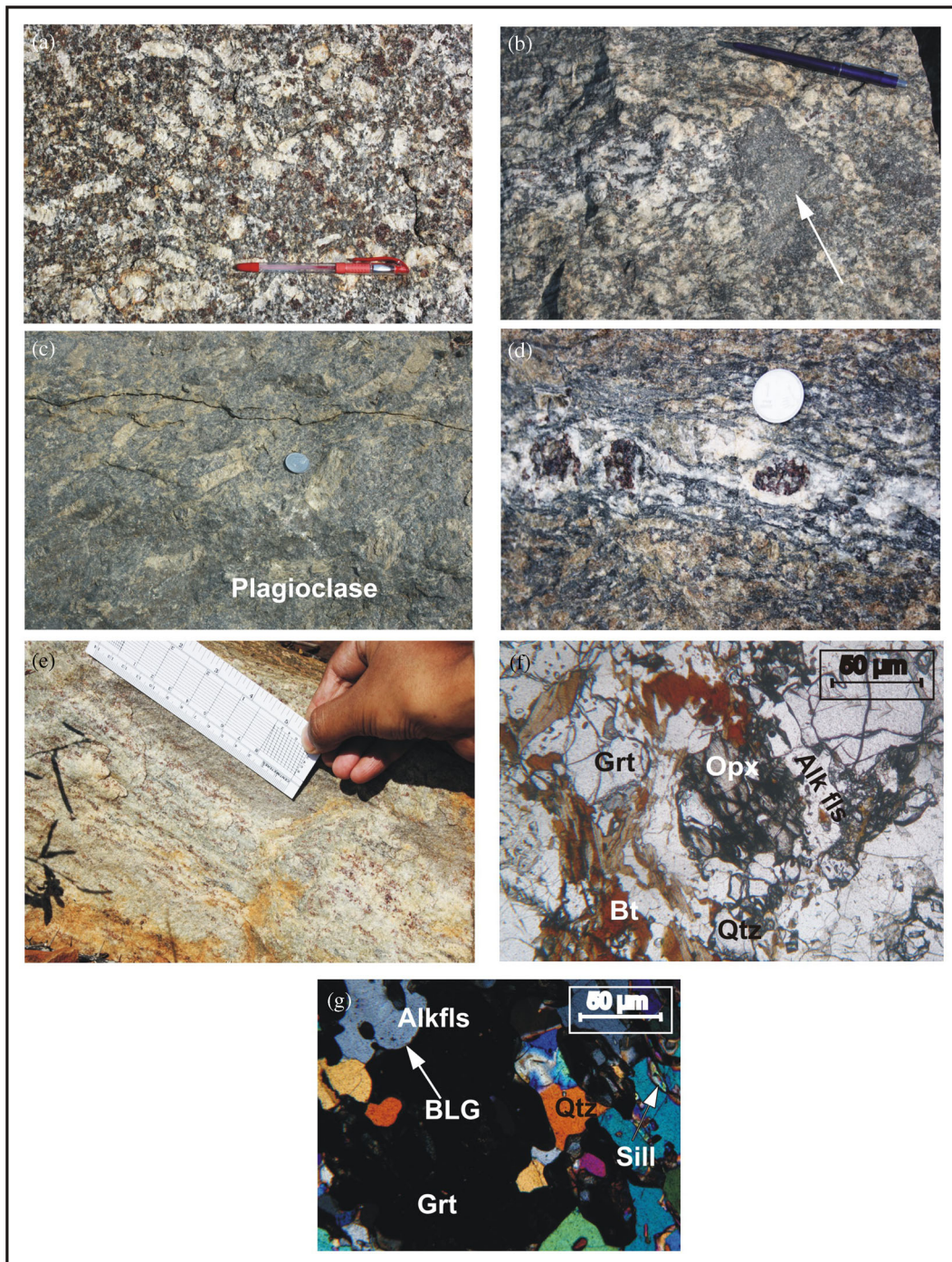
Figure 3. Mesoscopic and microscopic petrological characteristics of different rock types: (**a**) leucocratic variety of megacrystic with subhedral feldspar megacrysts in a matrix of biotite, feldspar and quartz with associated coarse garnet clasts. (**b**) Megacrystic leuco-granitoid with anhedral feldspar grains, quartzofeldspathic melt with matrix made up of garnet and biotite containing angular shaped mafic microgranular enclave (marked by arrow) with more or less sharp contact zone. (**c**) Euhedral to subhedral plagioclase in dark matrix of crudely foliated grey megacrystic granitoid. (**d**) Quartzofeldspathic mat surrounding garnet-rich clast (peritectic) in a deformed and sheared megacrystic graygranitoid. (**e**) Stretching lineation defined by garnet and biotite in leptynitic gneiss. (**f**) Coarse orthopyroxene (Opx) and garnet (Grt) grains are altered to retrogressive biotite in an orthopyroxene bearing migmatitic gneiss. The matrix shows occurrence of deformed alkali feldspar (Alk fls) and quartz (Qtz). (**g**) Bulging recrystallization (BLG) dominated deformation of alkali feldspar (Alk fls) at the contact of garnet (Grt) porphyroblast. Note the presence of quartz (Qtz) and sillimanite (Sill) needles in the matrix.

proportion of garnet porphyroblasts, opaque phase, and biotite. The concentration of quartz is variable in this leptynitic unit. Garnet porphyroblasts in leptynitic gneiss contain inclusions of biotite and quartz with occasional presence of opaque minerals. In the white leptynite, quartz forms

monocrystalline ribbon of L/W >10:1. Both the variants of leptynites are characterized by stretched and lineated garnet and opaque minerals 2–5 mm in length (figure 3e). In the grey leptynite, melanocratic layers consist 30–40% modal biotite, where the porphyroblastic garnet is concentrated both in cm scale biotite richer fraction and leucosomal quartzofeldspathic fraction.

There are broadly two varieties of charnockite in the host lithotypes. They are migmatitic charnockite and massive charnockite-enderbite gneiss. Migmatitic charnockite is a heterogeneous rock composed of alternate orthopyroxene, biotite, opaque phase, and minor garnet bearing melanocratic layers and leucocratic quartz, alkali feldspar, and plagioclase lath bearing layers in decreasing order of abundance in outcrop. The contact nature between the leptynitic gneiss and migmatitic charnockite is diffuse in nature. Porphyroblastic orthopyroxene develops boudins oriented along the gneissic foliation in the migmatitic charnockite. Alkali feldspars mostly dominate in between the polycrystalline quartz ribbons. The ribbons show length versus width ration (L/W) >6:1 and monocrystalline quartz ribbons with L/W <5:1 under microscope. Observed aggregate shape preferred orientation (ASPO) is the result of dynamic recrystallization. Coarse orthopyroxene and garnet are fractured and filled up with late biotite (figure 3f). Massive charnockite enderbitic gneisses are greasy melanocratic, heterogeneous rock with orthopyroxene, lesser amount of clinopyroxene, feldspar, quartz, and garnet. Discontinuous quartzofeldspathic aggregates of mm scale create diffuse gneissic pattern in this lithoytype with aggregate shape preferred orientation.

Khondalite is interbanded with quartzite in decimeter-scale to outcrop-scale. Khondalite is gneissic with alternate porphyroblastic garnet, biotite, sillimanite bearing fraction, and quartz, feldspar bearing fraction. Subgrains of alkali feldspar, garnet, and quartz show inequigranular interlocking texture. Alkali feldspar dominated matrix contains clusters of sillimanite. Quartz forms ribbons with aspect ratio >6:1 in some cases. Bulging recrystallization (BLG) mechanism dominates in the feldspars causing deformation processes in contact with garnet (figure 3g). They show very coarse sillimanite needles occurring disseminated and aligned parallel in the quartz-alkali feldspar matrix and somewhere create coarse aggregate. Garnets contain biotite, quartz, and opaque inclusions and are highly fractured. Quartzite shows foliation planes defined mostly by stretched and flattened quartz with garnet and biotite flakes. Opaque phases are present in both of them. There are khondalite lenses found within the leptynitic country rock in our study area.

Bands and lenses of melanocratic medium to coarse grained mafic granulite enclaves occur both in migmatitic gneisses, quartzites, and khondalites.

3. Geochemistry of granitoids

XRF analysis of selected samples of granitoids (leucocratic and grey variety) was done from National Centre for Earth Science Studies (NCESS), (Ministry of Earth Sciences, Government of India), Thiruvananthapuram by Bruker model S4 Pioneer sequential wavelength-dispersive X-ray spectrometer under pressed pellet and presented in table 1.

Both the varieties of granitoids, viz., leucogranitoid and grey granitoid were taken for geochemical classification. The oxide data of rocks were plotted in QAP diagram of Streckeisen (1974) after normalization on catanormal basis. Grey granitoids plot in the monzogranitic field along with the leucogranitoids (figure 4a). Some of the plots cluster at the granodiorite monzogranite boundary. Feldspar triangle plot devised by O'oconnor (1965) has also been utilized using CIPW basis to classify the rocks bearing >10% quartz based on feldspar ratios. Megacrystic leuco and grey granitoids are scattered in quartz monzonitic field (figure 4b). The mineralogy may coincide with K-rich granodiorite as discussed in O'oconnor (1965).

Plutonic coarse-grained rocks may be redefined using alkali content (Na_2O+K_2O wt%) against SiO_2 wt% diagram modelled by Middlemost (1994). Granitoids fall in the diagram on the subalkaline field (figure 4c) and are principally clustered around mean composition of granodiorite. The leucogranitoid shows much more compositional scatter than grey variety. The leucogranitoid plots from granodiorite to granite, whereas grey variety spreads from granodiorite to granodiorite-tonalite transitional composition. The granitoids are geochemically classified according to Frost *et al.* (2001). Ferroan index (figure 4d) denotes that both the granitoids are mostly ferroan in nature, although each of the respective variety falls in magnesian field. MALI (Modified alkali lime index) was defined by Frost *et al.* (2001) to match common plutonic compositional trends with calcic, calcalkalic, alkali-calcic, and alkalic trends. For any given suite of rock MALI increases with increasing SiO_2 wt%. When plotted, this index shows a crude trend of the granitoids from calcic to calc alkali field (figure 4d). This trend is much stronger for the megacrystic charnockite. Granitoids are plotted in ASI versus A/NK diagram (figure 4d). Aluminium saturation index (ASI) defines the molecular ratio $Al/(Ca−1.67P+Na+K)$ (Frost *et al.* 2001). Corundum normative is indicated for ASI >1 for excess aluminium that is not

Table 1. *Major elements (wt%) and trace elements (ppm) composition of megacrystic leuco- and grey-granitoids from study area.*

Sample no.	PV179A	PV203	PV137	PV159	PV10D2	PV220	PV166
Lithology	Megacrystic leuco-granitoid				Megacrystic grey-granitoid		
SiO_2	67.81	74.469	67.17	68.22	65.24	65.36	65.7
TiO_2	0.86	0.258	0.84	1.14	1.8	1.14	0.63
Al_2O_3	15.07	13.581	14.66	13.76	12.55	15.07	15.73
MnO	0.06	0.03	0.07	0.09	0.14	0.11	0.05
Fe_2O_3	4.38	1.817	4.85	5.94	8.27	6.3	4.73
CaO	4.34	2.082	2.96	4.02	4.73	3.77	3.29
MgO	1.18	0.223	0.94	0.77	1.05	1.17	1.56
Na_2O	1.79	2.473	1.67	1.95	1.95	1.7	1.56
K_2O	3.54	4.47	5.82	3.25	3.23	4.53	5.58
P_2O_5	0.2	0.066	0.31	0.37	0.72	0.39	0.26
V	67	25	50	65	72	78	64
Cr	ND	17	ND	3	ND	17	21
Co	23	5	21	27	34	25	23
Ni	8	6	7	4	ND	11	17
Ga	19	ND	14	14	14	14	16
Rb	165	56	231	103	68	155	178
Sr	242	429	207	158	138	274	322
Y	36	77	46	40	98	71	20
Zr	342	48	366	443	618	422	275
Nb	17	190	18	25	52	23	4
Ba	0.11%	31	0.14%	635	480	0.16%	0.23%
La	128	245	94	78	118	86	169
Ce	232	12	169	137	229	153	287
Sm	12	48	9	10	13	8	14
Th	52	57	13	1	ND	ND	74
L.O.I.	0.51	0.47	0.40	0.22	0.04	0.14	0.47

Note: Error in Ga content is ± 0.4 ppm except for one sample (4 ppm). ND: Below detection limit.

accommodated in feldspar. Aluminous minerals like muscovite, sillimanite, and garnet are present in the rocks because of strongly peraluminous nature of the rocks. Ca would be excess in rock that could be accommodated in feldspar when ASI <1 and $(Na + K)/Al$ <1.0. Therefore, phases like calcic amphibole or calcic pyroxenes may be present in the rocks. For ASI<1 and $(Na+K)/Al$>1.0, the rocks would have excess alkali element than could be accommodated in feldspars. ASI versus A/NK plots signify metaluminous to weakly peraluminous character for grey granitoids and weakly peraluminous nature of the white granitoids. Grey granitoids show higher modal proportation of amphibole and pyroxene. Ga-enrichment discrimination diagram (Whalen *et al.* 1987) has been used to classify the granitoids (figure 4e). However, the employed analytical method has major uncertainty in the Ga content. Thus, the granitoids are more or less calcic to calc alkaline, metaluminous to weakly peraluminous suite of rocks, which shows iron enrichment and possibly originated as I- and S-type in character.

4. Imprints of structural fabrics in regional scale

The planar and linear structural elements, which are key indicators for deciphering the structural evolution of that have been studied systematically and are illustrated in figure 5. The detailed structural mapping was carried out in 1:50,000 scale covering approximately 450 km^2 (figure 5). The area exposes with granitoid rocks hosted in a suite of granulite rocks. The primary sedimentary banding S_0 could not be identified in metasediments like quartzite-khondalite units in host granulites either in outcrop-scale or under microscopic study. Therefore, deformational signatures related to transformation from S_0 to S_1 are completely lost due to successive deformation and high-grade metamorphism producing partial melting. The S_1 fabric is rarely preserved in the host migmatitic gneisses in outcrop-scale, which is a product of D_1 deformation. The development of S_1 fabric and subsequent folding of it producing earliest recognizable F_1 fold in D_2 deformation are only
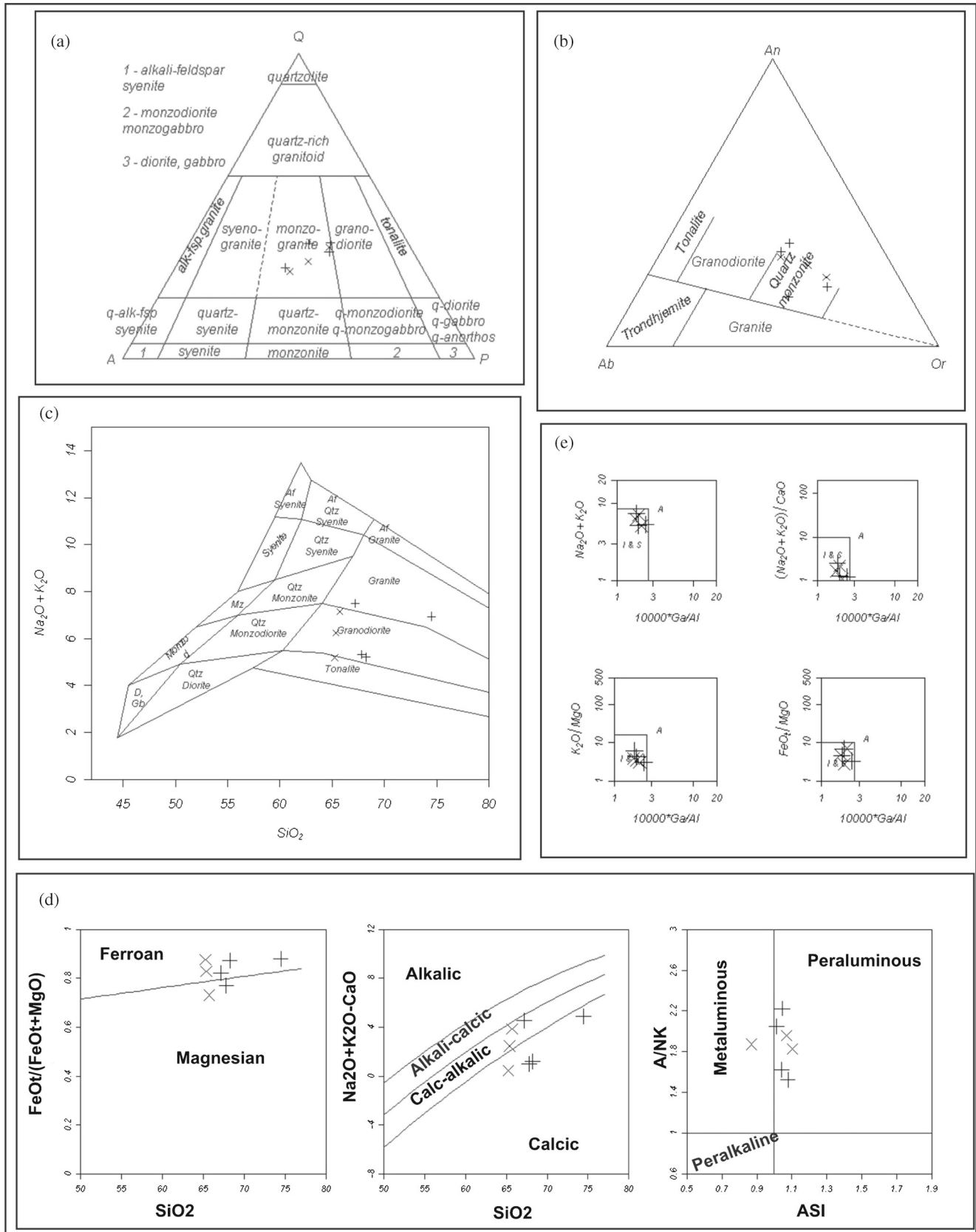
Figure 4. (**a**) Representative analysis defined in diagram of Streckeisen (1974). Megacrystic leucogranitoid is shown in by +, grey megacrystic granitoids by x. The data for all the analyses used in the diagrams are given in table 1. (**b**) Analytical data plotted in feldspar triangle plot (O'oconnor 1965). (**c**) TAS diagram plotted with representative analysis defined by Middlemost *et al.* (1994). (**d**) Classification diagram of Frost *et al.* (2001) with similar notation with representative samples (a). (**e**) Representative samples classified by Whalen *et al.* (1987) with same notation used as (a).
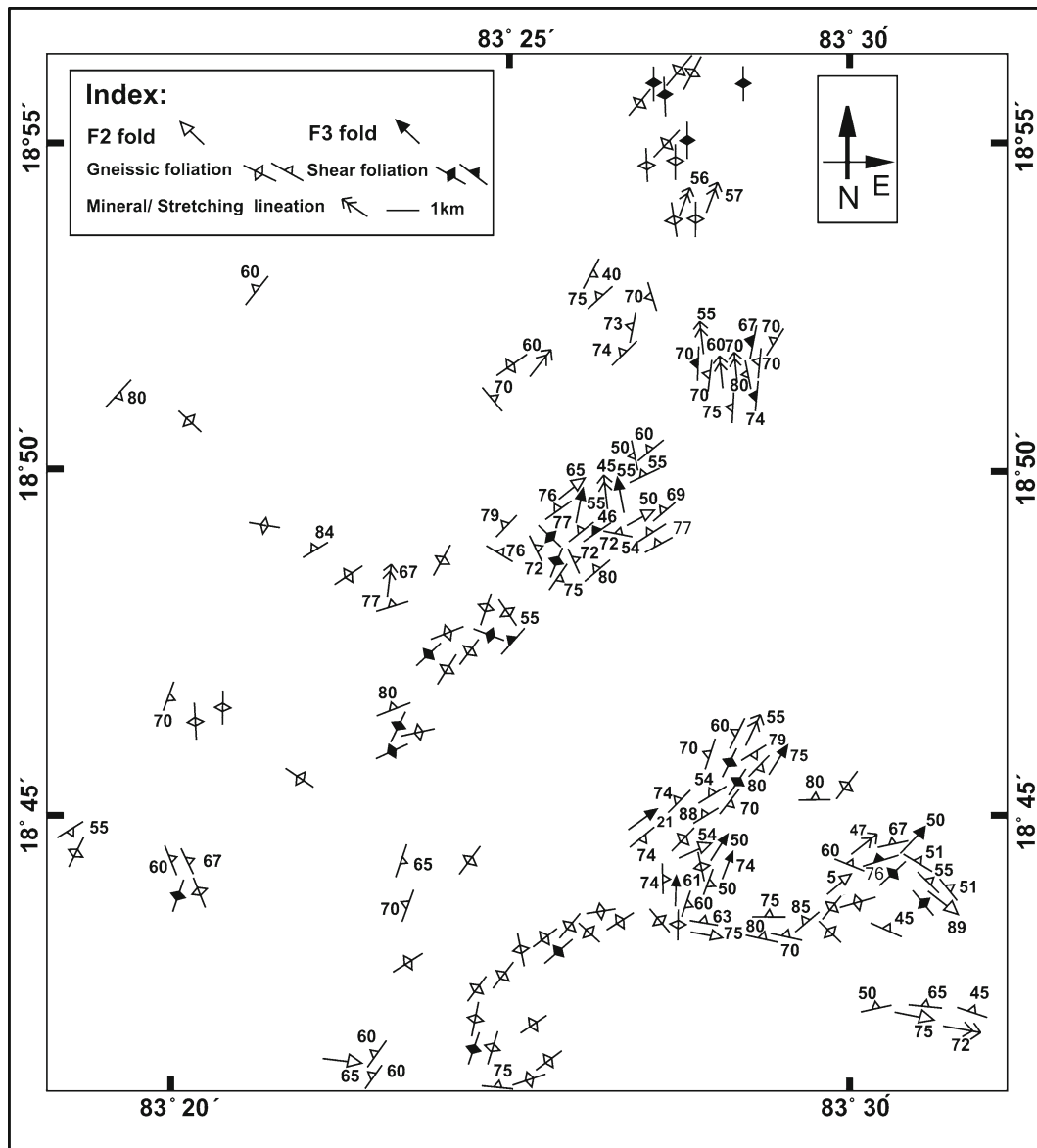
Figure 5. The structural map of the study area showing different structural fabrics and lineations, originally mapped on 1:50,000 scale.

preserved in the outcrop-scale and will be discussed further in next section. The characteristic gneissic foliation occurs as regional penetrative planar fabric in all host granulites, which is designated here as S_2 in D_2 deformation. Granitoids bear earliest fabric as crude gneissosity, which is conformable to this S_2 gneissic foliation in the host migmatites and hence the granitoids may be referred to as post S_1 intrusion. The gneissic foliation mostly trend northeast–southwest in the southern part and swings to north–south in the northern part. The foliations have moderate to steep dip, and in several places it is nearly vertical. Absence of any marker units and only presence of gneissosity in granitoids and associated granulites make the interpretation of structural disposition very difficult. For better understanding and

representation of the regional structural disposition, the strike line sketch map has been prepared (figure 6). The quartzite-khondalite unit enveloped with banded migmatitic gneisses and granitoids in the southern part have been tightly folded (F_2) in regional scale with broad northeast–southwest axial trace. The S_2 gneissosity, the form surface of the tight F_2 fold, has been transposed tectonically with the axial plane of the F_2 fold and locally the planar fabric exhibits transposed S_2/S_3 gneissosity. The overall regional fold pattern represents an upright to steeply inclined with vertical to steeply plunging synform. The axial plane of the regional fold is curved implying a superposed nonplane folded structure due to subsequent deformation. The axial trace of this later fold (F_3) roughly strikes along north–south with fold axis plunging
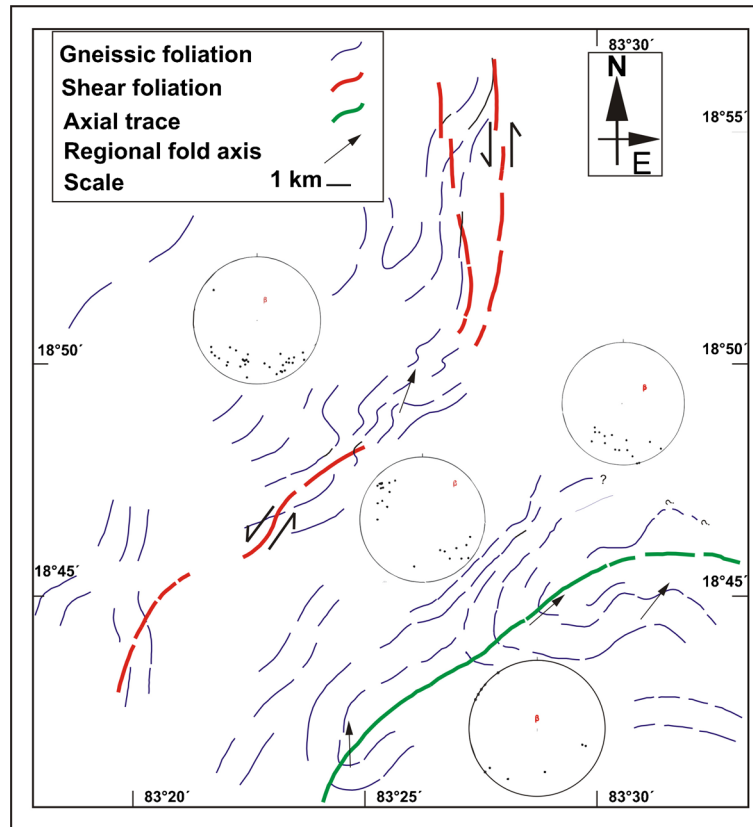
Figure 6. Sketch map showing the systematic variation and relationship of different generations of planar fabrics. Sectorwise β-diagrams are included in the map.

towards NE. The sectorwise β plot of the gneissosity (S_2) demonstrate how the fold axis of regional F_2 has been modified with later deformation. The regional modified F_2 (or F_3) changes its attitude from vertical (plunge 80°) to 23° → 41° and finally it plunges 55° towards 54°. The systematic variation of the fold axes reveals the nature of superposed structure as non-plane non-cylindrical fold. However, the other part of the study area is covered with crudely foliated granitoids and preserve less discernible fold structures except for a few asymmetric to tight folds. The S_2 gneissic foliation deforms differently and strikes broadly northeast–southwest to north–south direction and locally preserved fold structure. The regional-scale anastomosing shear zone with prominent sinistral sense cuts across the earlier folded S_2 gneissic foliation in the granitoids and migmatitic gneiss that runs from north toward south through granitoids and swings towards south-southwest in southern part of the study area through granitoids and migmatitic gneiss. The imprints of mylonitic foliation on earlier gneissic foliation S_2 in this shear zone suggest a separate deformation after F_2. These shear foliations are either vertical or steeply dipping (∼70°) towards west to northwest with conspicuous steeply plunging stretching lineation. Few dextral

shear bands oriented either along NE–SW trend or E-W trend conjugate in nature with the dominant mylonitic foliation, dipping westerly to vertical, have been observed in outcrop-scale.

5. Development of structural elements from mesoscopic to microscopic scale

Four episodes of deformational events have been studied in this, viz., D_1, D_2, D_3, and D_4. The earliest planar fabric recognized in the host migmatitic gneisses is S_1 which is the result of D_1 deformation. The deformational mechanism could not be deciphered either from outcrop studies or by microscopic investigation. Therefore, first recognizable fold, F_1 has been identified in the migmatitic gneisses on S_1 in D_2 event. F_2 and F_3 folds are developed in D_3 and D_4 deformation respectively. D_1 and D_2 deformations have been studied in meso- to microscopic scale whereas the D_3 and D_4 have been studied from micro- to megascopic scale. D_1 and D_2 deformations are the product of prograde to peak metamorphic condition. However, D_3 and D_4 are the result of post-peak metamorphic condition.

5.1 D_1 event

First recognizable planar fabric, S_1, identified only in the host migmatitic gneisses is the thinly laminated quartzofeldspathic units (figure 7a), which may be predicted as incipient melting during prograde metamorphic (M_1) condition. Biotite–quartz–feldspar is the possible prograde mineral assemblage as deciphered from the inclusion texture within garnet in gneissic rocks. Microstructures, textures as well as mesoscopic structures relating to this prograde metamorphic history is completely lost and could not be quantified properly. Therefore, earliest S_1 fabric has been formed in D_1 event in pre-peak metamorphic condition in host migmatitic gneisses.

5.2 D_2 event

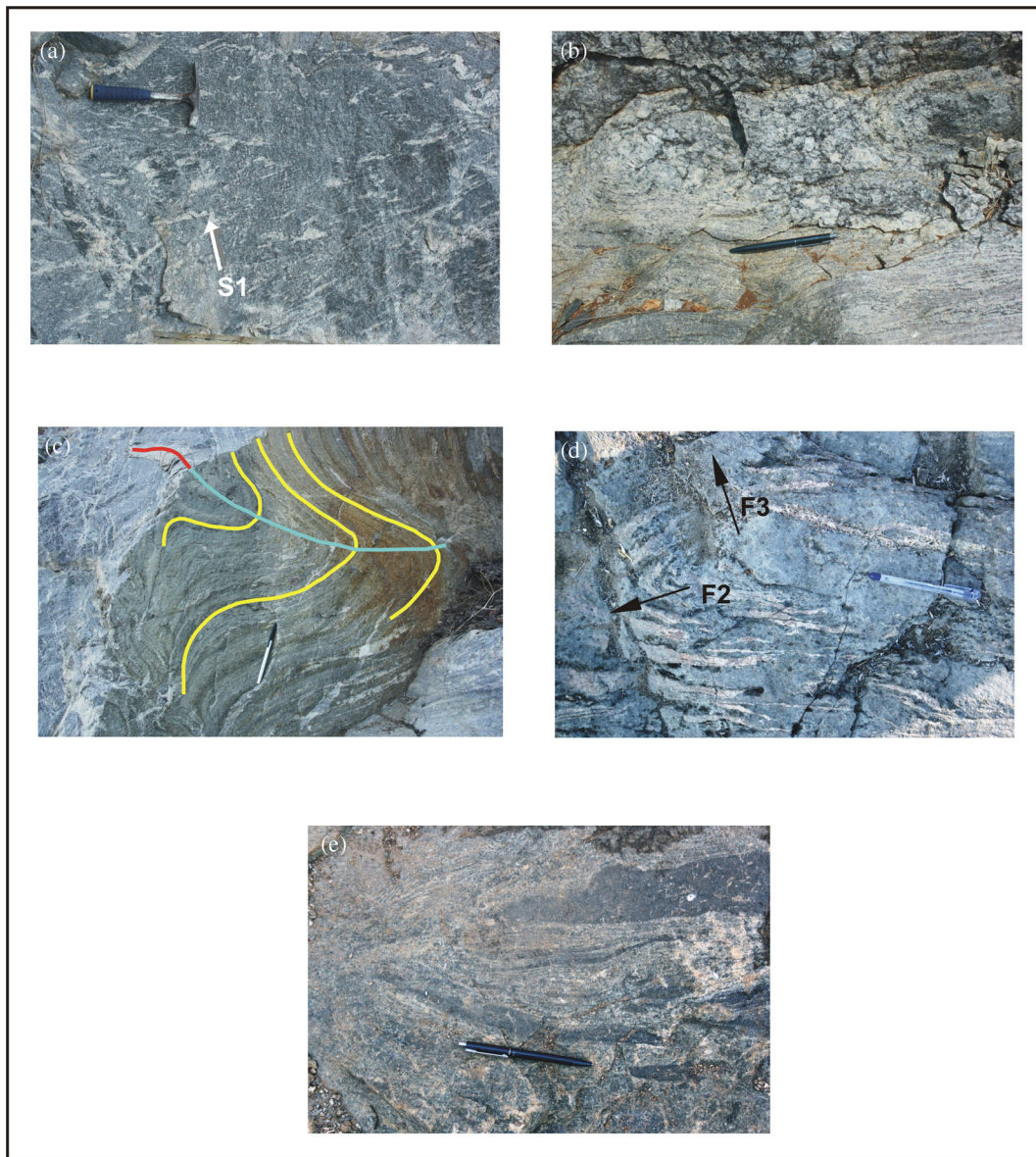The S_1 planar fabric has been deformed showing rootless tight to isoclinal F_1 folds (figure 7a) in D_2

Figure 7. Outcrop scale structural features in the lithotypes. (**a**) The S_1 compositional bands occuring in the form of rootless isoclinal folds in a host of migmatites, where the S_2 gneissosity is axial planar to the folded S_1 fabrics. (**b**) S_2 gneissic foliation in leptynitic gneiss and crudely foliated with stretched and flattened feldspar clasts having conformable relationship. (**c**) Non-plane superposed fold defined by S_2 gneissic foliation of quartzofeldspathic gneiss resulting from interference caused by D_3 and D_4 deformation. S_2 gneissic foliation and axial plane are marked in the figure. Note the curvature and modification of axial plane on vertical and on near horizontal plane. (**d**) Isoclinal folding on S_2 gneissic foliation of migmatitic gneisses showing F_2 and F_3 folds. (**e**) Tight to isoclinal fold on mafic bands parallel to the S_2 gneissic foliation of migmatitic gneiss. Mafic bands are boudinaged on the limb. Note that the S_2 foliation is transposed with the axial plane S_3.

deformation. The characteristic penetrative gneissic foliation S_2 has been developed in all the host granulites during D_2 deformation, which is axial planar to these rootless isoclinal to tight folds on S_1. The earlier fabric S_1 has been transposed with the axial planar foliation S_2. High-grade deformations accompanying partial melting have obliterated the earliest S_1 fabric and F_1 folds in the granulites. The F_1 folds on S_1 fabric are seldom preserved in the host migmatitic gneisses. As a result, S_2 gneissic foliation is the characteristic penetrative fabric in host granulites in meso- to megascopic scale. The gneissosity in migmatites is defined by garnetiferous mesocratic layers alternating with leucocratic quartzofeldspathic layers. In khondalites, on the other hand, S_2 fabric is characterized by alternate bands of mesocratic garnet-biotite-sillimanite bands and leucocratic quartzofeldspathic bands. Coarse grained megacrystic granitoids occur within migmatitic gneiss and quartzite-khondalites as massive to crudely foliated nature. Granitoids bear the earliest planar fabric as crude gneissic foliation, which is conformable with S_2 fabric in the host granulites. Plagioclase megacrysts and the matrix minerals in the well deformed granitoids are flattened and elongated showing a crude foliation, which is parallel and conformable with the S_2 foliation in the adjacent leptynitic gneiss (figure 7b). Thus the granitoids are deformed and metamorphosed and predictably emplaced pre- to syn-D_2 event.

Porphyroblastic garnets have been stabilized in granitoids and in leptynitic migmatitic gneiss in peak metamorphic condition (M_2). Garnet-sillimanite bearing assemblage has been stabilized in khondalite defining the gneissic foliation. S_2 gneissic fabric is defined by garnetiferous layers in garnet bearing granulites. Porphyroblastic garnets are mantled by the quartzofeldspathic mat in metagranitoids and associated leptynitic gneisses suggesting melt present peak metamorphic condition M_2 during D_2 deformation.

5.3 D_3 event

The pervasive gneissic foliation, S_2 in the host granulites and the crude gneissic foliation (S_2) in metagranitoids systematically varies in regional scale as discussed in the earlier section. In the southern part, the S_2 fabric in the successive litho units of khondalites, quartzites, migmatitic gneisses, and metagranitoids exhibit regional F_2 folding with NE–SW axial plane (figure 6). The regional folds are tight, gently to steeply plunging ($23° \rightarrow 55°$) to vertical and upright to inclined synform. The curved axial plane of this regional F_2 fold is the result of subsequent D_4 deformation,

which modified the F_2 fold axis differently producing non-plane non-cylindrical superposed folds. In the northern part, the folds are less discernable in regional scale on S_2 gneissic foliation and exhibit systematic strike variation of deformed S_2 from NE–SW to N–S direction. In outcrop-scale, the S_2 fabric is deformed exhibiting similar style of folding in host granulites. Near Ullibhadra, on near vertical surface the F_2 fold is evident on S_2 gneissic fabric. The S_2 gneissic layering in the leptynitic gneiss has been deformed forming inclined gently plunging folds (figure 7c). Axial plane (S_3) of this fold strikes $30°$ dipping $35°$ easterly. Attitude of the axial plane changes from inclined to horizontal orientation. Thus the axial plane of the F_2 fold is curved or folded again forming non-plane cylindrical superposed structure. Axial plane changes its dip from $35°$ to nearly $0°$. Fold axis is gently plunging NE. Near Gadabavalasa, S_2 gneissic foliation in migmatititc gneiss is isoclinally folded (F_2) and is transposed with newly developed axial planar fabric (S_3) forming a composite S_2/S_3 gneissic foliation (figure 7d). This F_2 fold is modified and deformed again by later deformation. The mafic bands within leptynitic gneiss has been refolded (F_3) where the transposed S_2/S_3 is axial planar to the fold (figure 7e). Commonly the F_2 fold axis plunges moderately towards east. However, fold axes show plunge variation in the range of $50°$–$75°$ towards NE to SE developing a non-cylindricity due to modification by subsequent deformation (D_4).

Microscopically the porphyroblastic phases in khondalites and leptynitic gneisses do not commonly show retrograde break down textures – characteristics of decompression and/or cooling event. However, the high Mg–Al rocks in other parts of EGB are susceptible to record any textures during retrograde metamorphic events (Sengupta *et al.* 1990, 1991; Dasgupta *et al.* 1994; Bhowmik *et al.* 1995). S_2 gneissic foliation, defined by porphyroblastic phases, developed during near-peak metamorphic condition are subsequently deformed during D_3 deformation. Porphyroblastic ferromagnesian phases in the host granulites are sometime replaced by late biotites (figure 3e) as discussed in earlier section. Therefore D_3 event may be referred to as post-peak metamorphic deformation.

5.4 D_4 event

D_4 deformation is characterized by the shear zone development in a compressional regime (transpression). Earlier axial plane of F_2 folds has been refolded forming superposed structure, which is the result of interference between F_2 and F_3. Regional F_3 fold axis plunges $55°$ towards $54°$ with axial trace along N–S. Systematic variation of F_2 fold

axis occurred due to modification of this fold axis and axial plane due to D_4 deformation. The superposed structures are evident in mesoscopic scale. At the southern part of the study area in regional scale modified F_2 folds show plunge variations (figure 5) and the axial plane of the regional fold has been curved (figure 6) developing non-plane non-cylindrical fold. Axial trace of this F_3 fold strikes broadly along N–S direction. Regional scale shear zones are developed in anastomose geometry with sinistral sense (figure 6).

Shear zone runs mainly through granitoids and hence, this is the main rock type, which is affected severely by the development of mylonitic fabric (figure 8a). However, the leptynitic gneiss and charnockite-enderbite gneiss are also affected by the development of high strain zones in outcrop scale. Mylonitic foliations are mostly vertical or steeply dipping ($\sim$70°) westerly that intersects the crude foliation of the metagranitoids. The feldspar megacrysts of granitoid gneisses in the shear zone are flattened and elongated forming
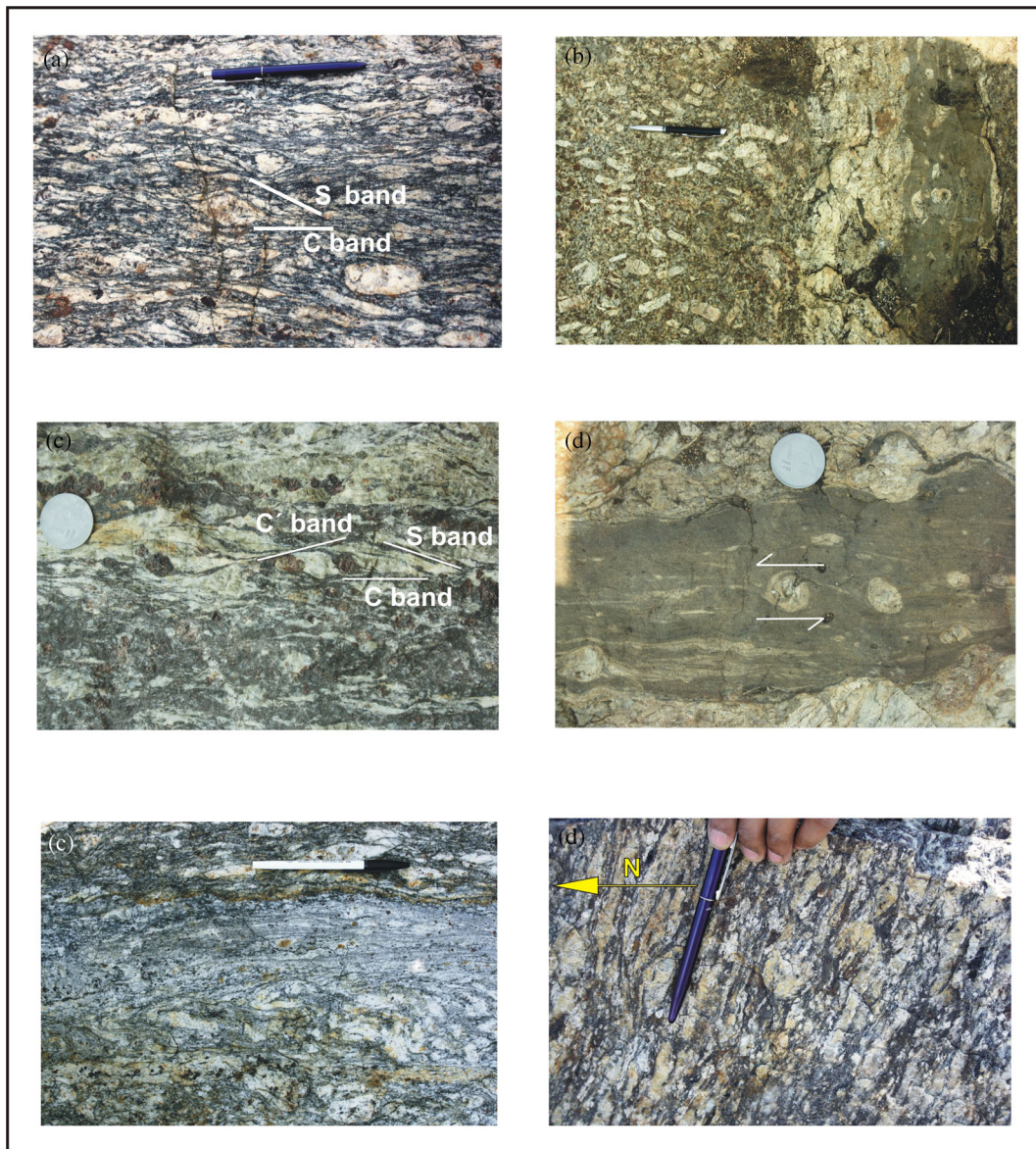

Figure 8. Structural features resulting from the development of shearing in migmatites and granitoid gneisses. (**a**) Mylonitic fabrics in leuco variety of granitoid gneiss showing S–C fabrics marked on it. (**b**) Ultramylonitic band crosscutting the crude fabric of granitoid gneiss. Note the development of augen-shaped feldspar clasts within fine grained dynamically recrystallized matrix in mylonite band at right part of the figure. (**c**) C–S–C' fabrics in mylonitic granitoid gneiss with Ω plagioclase and garnet clasts. (**d**) Asymmetirc ∂ clast of feldspar in an ultramylonitic shear band in granitoid gneiss suggesting sinistral shear sense. (**e**) Asymmetric shear folding in the shear bands of migmatitic gneiss. (**f**) Steeply plunging stretching lineation on subvertical mylonitic foliation in granitoid gneiss.

augen within the dynamically recrystallized matrix mineral grains producing finer aggregates (figure 8a). The strained feldspar clasts show the pancake shaped or oblate geometry when their axial ratio are plotted in the Flinn diagram (table 2). The values of X, Y and Z are given in table 2, where Z is the compressive axis, Y and X are the extensional axes. The table 2 shows the Flinn k value to be <1, which supports the strain parameters in a transpressional shear zone (Dewey *et al.* 1998; Fossen 2010). Stretching lineations are steep to subvertical in nature on the shear foliation (figure 5). Limited number of field data indicate kinematic vorticity number (Wk) to lie in the range of 0–0.81. Wk is a measure of ratio between pure shear and simple shear. Wk is measured with the angle between C fabric and S fabric (Ø) on the horizontal plane and the X–Z parameters of feldspar clasts in the granitoids following R_f-Ø method (Twiss and Moores 2007; Bo *et al.* 2009). The dynamically recrystallized ultramylonitic bands crosscut earlier gneissic fabric in granitoid gneisses (figure

8b). Depending on clasts/refined matrix ratio protomylonite, mylonite, and ultramylonite can be assigned (Ghosh 1993) for the sheared rocks. All the varieties are preserved in the area. Several shear sense indicators like S–C fabric, asymmetric shear fold, ∂ and Ω structures have proved useful. S-C, C-S-C', C-C' fabrics (figure 8c) are characteristic in the sheared granitoid gneisses, which suggest the sinistral sense of shearing. Both the ∂- and Ω-shaped feldspar clasts are preserved in the sheared granitoids (figure 8d). Asymmetric shear related folds are also a distinguishing feature in the shear zone (figure 8e) migmatites and as 'similar folds' in the granitoids (Ramsay 1967; Valentin 2000). All the structures of the shear zone suggest overall sinistral shear sense. Stretching lineation on the subvertical mylonitic foliation plunges moderate to steep (figure 8f) implying a dip-slip component in addition to the significant strike-slip component of shearing. Conjugate shears are also noticed where subvertical main shear zone strikes 45° with minor shear band trending E–W.

Table 2. *Axial parameters and calculation of corresponding Flinn k values of feldspar clasts in sheared granitoids. Z is the compressional axis whereas X and Y are the extensional axes. The parameters plotted in the Flinn diagram are shown here.*

Data no.	X	Y	Z	X/Y	Y/Z	ln(X/Y)	ln(Y/Z)	k value
1	5.7	5	1	1.140	5.000	0.131	1.609	0.035
2	5	5	1.7	1.000	2.941	0.000	1.079	0.000
3	6	6	2.1	1.000	2.857	0.000	1.050	0.000
4	8	7	2.5	1.143	2.800	0.134	1.030	0.079
5	6	6	2	1.000	3.000	0.000	1.099	0.000
6	4.7	3.3	1	1.424	3.300	0.354	1.194	0.184
7	6	6	2.1	1.000	2.857	0.000	1.050	0.000
8	8	7	2.5	1.143	2.800	0.134	1.030	0.079
9	6	3.8	1	1.579	3.800	0.457	1.335	0.207
10	7	3	1	2.333	3.000	0.847	1.099	0.667
11	4.5	4.5	1.6	1.000	2.813	0.000	1.034	0.000
12	6.9	6.5	1.5	1.062	4.333	0.060	1.466	0.018
13	6.7	4	1.2	1.675	3.333	0.516	1.204	0.289
14	7	5	1.5	1.400	3.333	0.336	1.204	0.171
15	8	7	2.5	1.143	2.800	0.134	1.030	0.079
16	4	3.5	1.1	1.143	3.182	0.134	1.157	0.065
17	5.3	4.5	1.2	1.178	3.750	0.164	1.322	0.065
18	6.9	6.5	2	1.062	3.250	0.060	1.179	0.027
19	6.7	5.7	1.8	1.175	3.167	0.162	1.153	0.081
20	8	6.9	2	1.159	3.450	0.148	1.238	0.065

Flinn diagram :
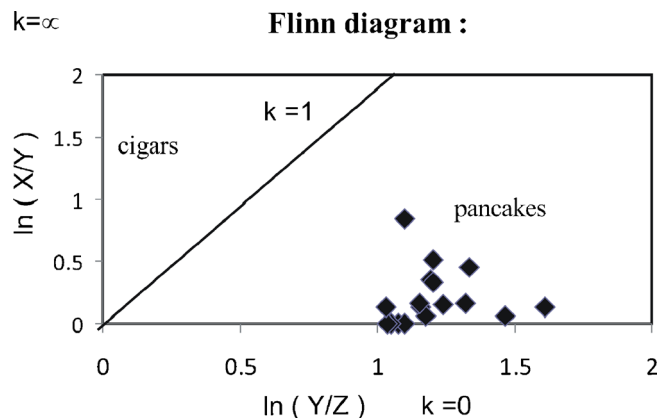
In outcrop scale, F_3 folds are developed on S_2 fabric in D_4 deformation. Both F_2 and F_3 folds are developed on same form surface S_2. Interference of F_2 and F_3 folds produces superposed fold structures. F_3 fold axes plunge 50°–80° towards N to NE. Variations of plunge suggest the modification of F_2 to F_3. Near Ullibhadra, axial plane of F_2 fold has been curved forming non-plane cylindrical fold (figure 7c). Near Gadabavalasa, F_2 fold on S_2 foliation has been modified with the development of F_3. F_2 fold on mafic band in the gneissic rock has also been refolded in this deformation.

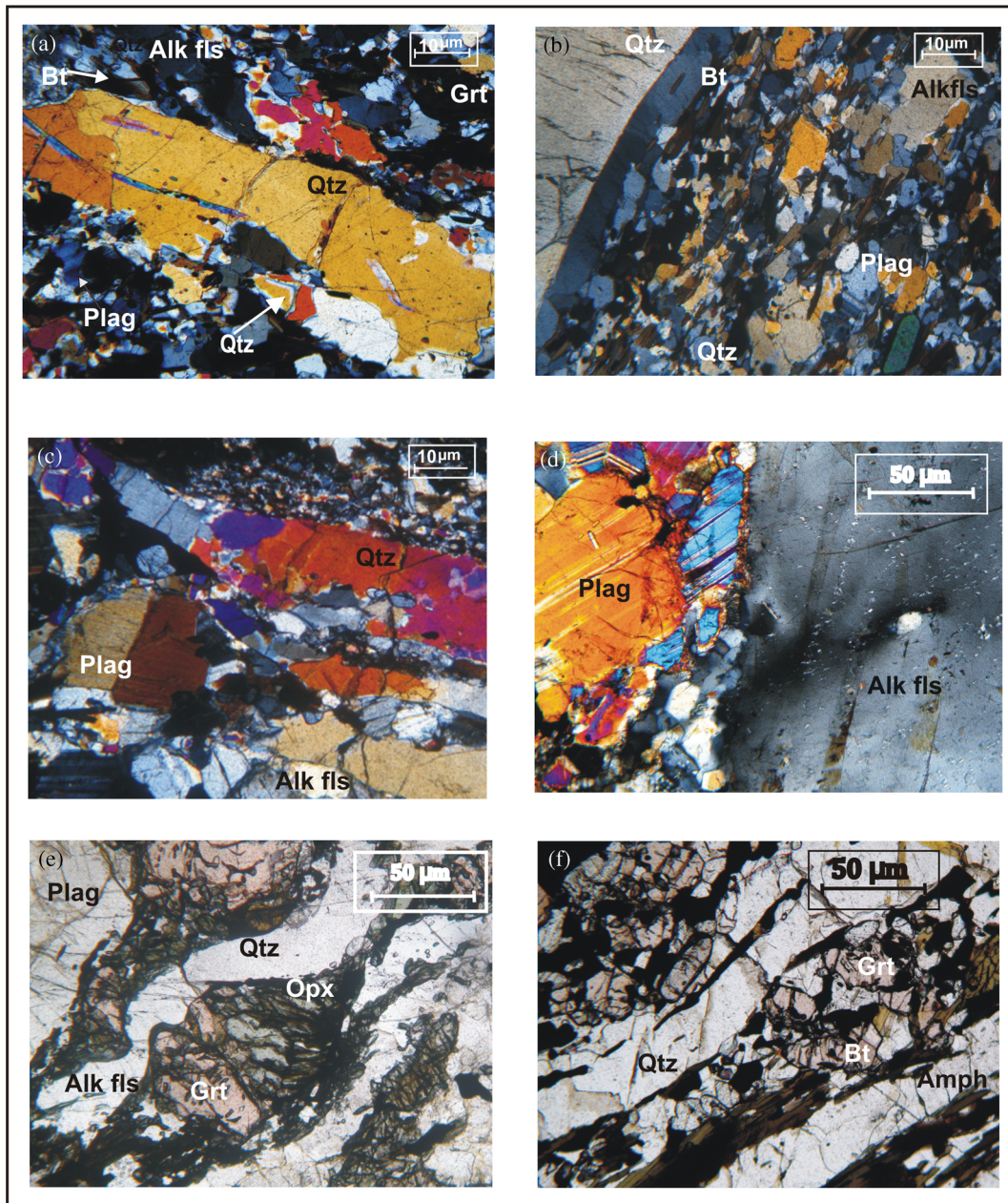Granitoids are classified based on intensity of development of mylonitic foliation and flattening of

Figure 9. Microstructural features in sheared granitoid gneisses. (**a**) Polycrystalline quartz (Qtz) ribbon in a matrix composed of dynamically recrystallized alkali feldspar (Alk fls), plagioclase (Plag), biotite (Bt) and garnet (Gt). (**b**) Deformed fabric forming quartzofeldpathic matrix minerals like quartz (Qtz), plagioclase (Plag) and alkali feldspar (Alk fls) grains with serrated grain boundaries with biotite flakes indicating subgrain rotation in a mylonitic granitoid gneiss. (**c**) Flattened and recrystallized quartz (Qtz) grains with subgrain formation and developing ribbons. (**d**) Plagioclase (Plag) and alkali feldspar (Alk fls) clasts showing deformation twinning and subgrain formation at the grain boundary in a less sheared granitoid gneiss. (**e**) Garnet (Grt) and orthopyroxene (Opx) porphyroblast wrapped up by quartz (Qtz) ribbon in a deformed matrix containing alkali feldspar (Alk fls), plagioclase (Plag) and quartz (Qtz). (**f**) Fractured Garnet (Grt) porphyroblast containing biotite (Bt) and quartz (Qtz) inclusions are replaced by late biotite (Bt). Note the presence of amphibole (Amph) in the matrix.

clasts and matrix minerals and grain refinement as unsheared, less-sheared, and highly-sheared varieties (Platt and Behr 2011; Passchier and Trouw 2005; Hippertt *et al.* 2001). The unsheared, less-sheared, and highly-sheared varieties are spatially distributed in the terrane when approaching towards regional scale or outcrop scale shear zones. Different stages of crystal-plastic deformation are preserved in sheared granitoids, which are the main mechanisms for grain refinement processes and mylonitic fabric development. Sheared granitoids are sometimes characterized by alternating leucosomal and melanosomal fractions. The leucosomal fraction is composed of large inequigranular interlobate texture composed of alkali feldspar, and plagioclase feldspar clasts (figure 9a) in a matrix of dynamically recrystallized quartz, alkali feldspar, and plagioclase relict. Plagioclase feldspar clasts develop augen texture with relatively undeformed core and surrounding recrystallized grains at the rim to sigma type mantled objects with deformed core. Monocrystalline quartz ribbon of aspect ratio >7:1 is observed. These grains show sweeping extinction. However, polycrystalline quartz ribbons with L/W >10:1 with development of subgrains (figure 9a) are also noticed. The ribbons occur along the shear foliation. Most feldspar grains in the matrix show typical subgrain rotation (SGR) associated to climb (figure 9b). Ultramylonitized bands are composed of quartz, alkali feldspar, and plagioclase in decreasing order of abundance. Quartz grains suffer crystal plastic deformation as indicated by the undulose extinction and subgrain formation (figure 9c). Feldspar grains in relatively undeformed rock contain deformation twin and BLG dominated grain boundary migration (GBM) process associated with subgrain formation (figure 9d). Inequigranular interlobate plagioclase grains with L/W $\leq$ 5:1 form subgrains and deformation twinning. Alkali feldspar grains form ribbon-like texture with L/W ratio of 4:1–5:1. Hydrous minerals like biotite and amphiboles are developed and oriented along the shear bands. Garnet, orthopyroxene, biotite, and amphibole grains are stretched along the shear foliation (figure 9e). Orthopyroxene grains are stretched along the shear foliation showing weak undulose extinction and deformation lamellae. They are bordered by finely recrystallized quartzofeldspathic matrix with serrated plagioclase grains having deformed twin lamellae. Amphiboles are recrystallized along grain boundary with deformed rotated lamellae. Porphyroblastic garnets are rimmed by feldspar and quartz intergrowth. The former grains occur within the quartzofeldspathic melt fraction exhibit fractures and BLG with the feldspathic melt. Well-developed fractures in garnet grains are filled up by biotite and opaque phases (figure 9f).
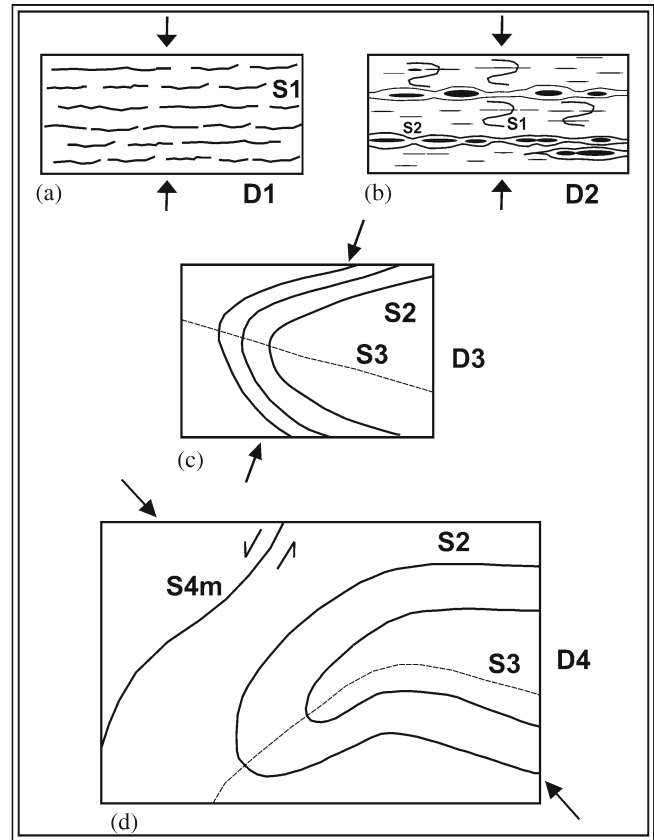

Figure 10. Schematic diagram showing the chronological development of the structural fabrics throughout the deformation events. (**a**) Development of S_1 fabric D_1 event during prograde metamorphic condition. (**b**) Development of S_2 gneissic fabric with porphyroblasts which is axial planar to the rootless folds (F_1) on by S_1 during deformation event D_2 during peak metamorphic condition. (**c**) Post-peak D_3 event causing deformation and folding (F_2) of S_2 gneissic fabric and development of S_3 fabric axial planar to the F_2 folds in local scale. (**d**) Development of sinistral shear zones and superposed non-plane non-cylindrical folding resulting from a bulk compression at an angle to the shearing in D_4 event.

The grain boundaries show bulging and are serrated in nature suggesting relatively high-T GBM mechanism and generate interlobate inequigranular texture. Smaller garnets show L/W ratio of 4:1–3:1 in mylonitic shear bands. Quartz ribbons and recrystallized quartzofeldspathic matrix grains wrap around the porphyroblastic garnets (figure 9e).

6. Discussion

The polydeformed polymetamorphed Domain 2 (Visakhapatnam Domain) of EGB suffered anticlockwise metamorphic P–T trajectory (Sengupta *et al.* 1990, 1991; Dasgupta *et al.* 1994; Karmakar *et al.* 2009 and references therein). Our detailed structural study suggests four distinct petrotectonic events (figure 10). D_1 event refering to
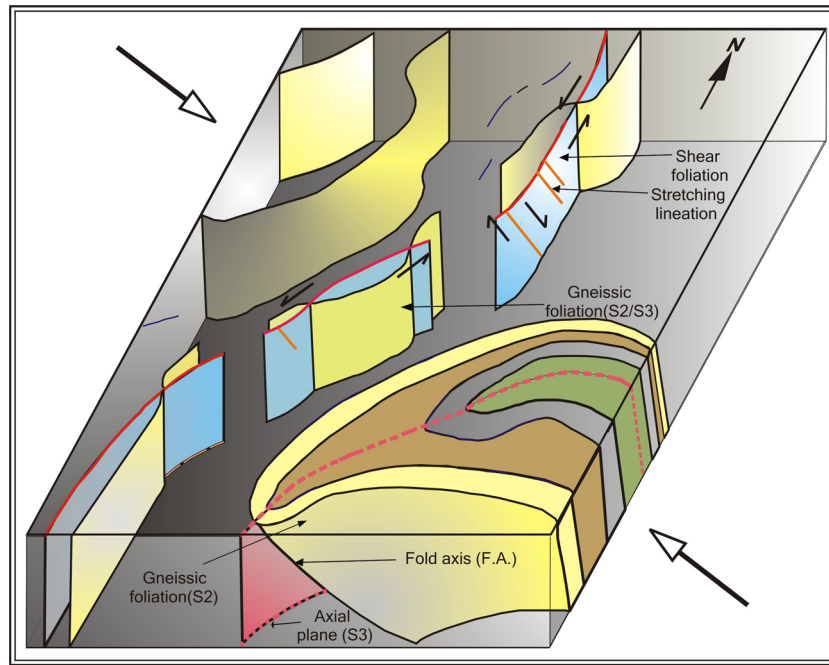
Figure 11. Schematic three dimensional block diagram showing present structural disposition of the area after D_4 event. Shear sense is marked on the shear foliation both on horizontal outcrop section and on vertical foliation along stretching lineation with a compressive force broadly along northwest–southeast direction. Western part is up-thrown block relative to the eastern part.

the prograde M_1 history of metamorphism and transformation mechanism from primary layering to S_1 is now obliterated. The event is possibly the initiation of high-grade metamorphism as evident from development of thinly laminated quartzofeldspathic units in migmatitic gneiss (figure 7a) resulting incipient partial melting (described in section 5.1). However, detailed characterization and the timing of prograde event in other parts of Domain 2 still remain inconclusive (Sengupta *et al.* 1990; Dasgupta *et al.* 1994; Das *et al.* 2011). The granitoids got emplaced during pre-peak to peak metamorphic condition, i.e., pre- to syn-D_2 event.

The granitoids are monzogranitic to granodioritic type based on normative classification and are of subalkaline nature (Middlemost *et al.* 1994). The metaluminous to peraluminous character (figure 4d) and I- and S-type nature of granitoids indicate a continental arc to collisional set up of emplacement probably related to active continental margin (Barbarin 1999). Two different mineralogical assemblages for grey and leuco granitoids (described earlier in section 2) with weak dissimilar trends in calcic to calc alkaline nature (figure 4d) in granitoids suggest evolution of two suites of rocks.

Development of S_2 gneissic foliation defined by porphyroblatic garnets in granitoid gneisses is conformable with the pervasive regional gneissic foliation (S_2) in the associated migmatitic gneisses and khondalites. D_2 event is therefore referred to as porphyroblastic garnet forming peak metamorphic granulite grade M_2 event. The peak granulite

event is characterised from Mg–Al rocks and other granulites in other parts of EGB (Sengupta *et al.* 1990, 1991; Karmakar and Fukuoka 1992; 1998; Bose *et al.* 2000, 2009; Das *et al.* 2011, 2012, 2013; Dasgupta *et al.* 1994). The granitoid gneisses bear the signatures of peak porphyroblasts development event with partial melting. D_3 event deforms this S_2 gneissic foliation at post-peak metamorphic condition and exhibits outcrop to regional scale F_2 folding. The D4 event is characterized by (i) presence of superposed fold structure; (ii) development of vertical to near vertical mylonitic foliation in regional and outcrop scale; (iii) steeply plunging stretching lineation; (iv) value of Flinn k ranging between zero and 1; and (v) kinematic vorticity number (Wk) <0.81. It can be ascertained from the above evidences that the shear zone in our study area is mostly of pure shear dominated transpressional regime (Fossen *et al.* 1994). So, D_4 is characterized by transpression with bulk shortening broadly along NW–SE direction (figure 10d). The resultant structure is illustrated using a schematic three dimensional block diagram (figure 11). In transpression the convergence vector is not orthogonal relative to the deformation zones in tectonic scale (Fossen *et al.* 1994; Dewey *et al.* 1998; Goscombe *et al.* 2003). The event is indicated by the development of anastomosing shear zones with superposed fold structures. Transpressional tectonics is instrumental in understanding the relative motion of crustal sections studied from different parts of the world (Ave Lallement 1997; Goscombe

et al. 2003) and is said to be an inevitable result of plate motion on a spherical surface (Dewey *et al.* 1998). Coupled interference of pure shear and simple shear stresses generates this situation in crustal rocks in compressional regime (Fossen *et al.* 1994; Fossen 2010). Pure shear acts to generate shortening normal to the shear zone and the asymmetricity in rocks and minerals are related to simple shear deformation. The transpressive zones always show noncoaxial strain pattern. In our area, structural studies imply sinistral motion of shearing with eastern part moved downward relative to the western part as upthrown block as suggested by shear sense indicators and stretching lineation (figure 11). Regional scale shear zones are confined within granitoids and leptynitic gneisses. However, other rocks including massive charnockites register development of micro shear bands with influence of regional high-strain zones. The coarse-grained quartzofeldspathic rocks like megacrystic granitoids and leptynites were probably rheologically susceptible to accommodate high-strain zones. Hydrous minerals like biotite and amphiboles are developed along the shear bands. However, large-scale melting and decompression textures are not apparent suggesting this reworking event takes place possibly without significant upliftment.

Mukhopadhyay and Bhattacharya (1997) illustrated the emplacement of granitoid syntectonically during prograde to peak metamorphic condition whereas the shearing is suggested as post-peak event. On the contrary, Chetty *et al.* (2003) inferred the granitoid emplacement at a much later event during development of shear zones. Chetty (2001) interpreted the EGB as collage of juxtaposed terranes (?) demarcated by the lineaments based on Landsat imagery data and suggested to fit a thrust tectonic, allochthonous model of amalgamation and accretion. Dasgupta *et al.* (2013) argued that the central EGB witnessed a prolonged accretion-collision history initiated at 1.5 Ga and culminated at ca 0.90 Ga with the formation of supercontinent Rodinia. The Domain 2 is bounded by the NSZ–VSZ lineament at northeast with Domain 3 and by Sileru shear zone (SSZ) at east with Domain 1B. However, present study area falls within the Nagavalli shear zone (NSZ) and our study reveals that the shear zones pass through granitoid gneisses. Sharp intrusive nature of granitoids apparent from the field relation clearly suggests that the megacrystic granitoids and charnockites intruded the package of rocks comprising migmatitic gneisses, charnockite-enderbites, quartzites, and khondalites. The host granulites are metamorphosed and deformed in the same manner as reflected from their petrological and structural studies described earlier. Chetty *et*

al. (2003) suggested thrust tectonics from development of flat to moderately dipping D_1 gneissic foliation (prior to the development of shear zones) from the present study area and correlated it with Archaean tectonothermal event based on Sm–Nd and Rb–Sr data from Domain 4 by Bhattacharyya *et al.* (2004). However, Simmat and Raith (2008) bracket early ultra-high temperature metamorphism within 1250–1100 Ma (M_1) using monazite chemical age data in khondalites and aluminous granulites and fabric defining granulites facies metamorphism (M_2) and anatexis in metapelites and felsic granulites between 980 and 940 Ma, synchronous with the intrusion of megacrystaic granitoids in EGP. In a recent study, UHT metamorphism in Domain 2 is demonstrated as occuring during 1.03–0.99 Ga using U–Pb zircon SHRIMP data (Bose *et al.* 2011; Das *et al.* 2011). The present study suggests that D_2 is the major pervasive fabric (S_2 gneissic foliation) forming event and reflects the peak metamorphic condition (M_2). However, systematic geochronological study is required to correlate this peak metamorphic event of the area with the recorded M_2 event of EGB. Chetty *et al.* (2003) speculated that the D_2 deformation corresponds to the development of a network of steep shear zones such as Sileru Shear Zone (SSZ), Nagavalli Shear Zone (NSZ), and Vamsadhara Shear Zone (VSZ). Over a period of 1450–850 Ma, granitoids got emplaced syntectonically with this D_2 deformation. However, it needs to be substantiated by the systematic geochronological data. They inferred NSZ–VSZ joins up with Rayner–Napier boundary shear zone in Antarctica. Present petrotectonic studies (shear zone forming D_4 event) indicate the mylonitic foliation overprinted the S_2 gneissic foliation of granitoids that emplaced before this event at pre- to peak metamorphic condition. This, in combination with already discussed isotopic investigations, in contrast suggests that the development of shearing may be younger than 1.03–0.99 Ga. It is reported by Chetty *et al.* (2003) to show the dextral shear sense. However, Mukhopadhyay and Basak (2009) argued that dextral motion is not kinematically compatible with regional framework of EGB. Our detailed structural studies invoke sinistral motion of shearing with eastern part as downthrown block relative to the western part as upthrown block. From the sequential development of transposed planar fabrics and superposed fold structures revealed from regional, outcrop and microstructural studies in four distinct events (D_1–D_4), we suggest that the granitoids emplaced at pre- to syn-peak metamorphic condition (pre- to syn-D_2 event) in the terrane and experienced compressional tectonics with transpression at D_4 due to oblique collision directed broadly towards

NNW manifested by development of sinistral shear zones.

References

Ave Lallement H G 1997 Transpression, displacement partitioning, and exhumation in the eastern Caribbean/South American plate boundary zone; *Tectonics* **16** 272–289.

Barbarin B 1999 A review of the relationships between granitoid types, their origins and their geodynamic environments; *Lithos* **46** 605–626.

Bhadra S, Gupta S and Banerjee M 2004 Structural evolution across the Eastern Ghats Mobile Belt–Bastar Craton boundary, India: Hot over cold thrusting in an ancient collision zone; *J. Struct. Geol.* **26** 233–245.

Bhattacharyya S, Swain A K and Teixeira W 2004 Crustal source for a syenite complex in the high-grade Eastern Ghats belt, India: Sm–Nd isotopic evidence; *Gondwana Res.* **7** 627–629.

Bhowmik S K, Dasgupta S, Hoerness S and Bhattacharya P K 1995 Extremely high temperature calcareous granulites from the Eastern Ghats, India: Evidence for isobaric cooling, fluid buffering and terminal channelized fluid flow; *Eur. J. Mineral.* **7** 689–703.

Biswal T K, De Waele B and Ahuja H 2007 Timing and dynamics of the juxtaposition of the Eastern Ghats Mobile Belt against the Bhandara Craton: A structural and zircon U–Pb SHRIMP study of the fold-thrust belt and associated nepheline syenite plutons; *Tectonics* **26** 1–21.

Biswal T K and Sahoo D 1998 IRS-1C Digital data interpretation of lithotectonic setting in northwestern part of the Eastern Ghats Mobile Belt, Orissa; *Curr. Sci.* **75** 846–850.

Bo Z, JinJiang Z, DaLai Z and Lei G 2009 Strain and kinematic vorticity analysis: An indicator for sinistral transpressional strain partitioning along the Lancanjiang shear zone, western Yunnan, China; *Science in China Series D: Earth Sci.* **52** 602–618.

Bose S, Das K, Ohnishi I, Torimoto J, Karmakar S, Shinoda K and Dasgupta S 2009 Characterization of oxide assemblages of a suite of granulites from Eastern Ghats Belt, India: Implication to the evolution of C–O–H–F fluids during retrogression; *Lithos* **113** 483–497.

Bose S, Dunkley D J, Dasgupta S, Das K and Arima M 2011 India–Antarctica–Australia–Laurentia connection in the Paleo-Mesoproterozoic revisited: Evidence from new zircon U–Pb and monazite chemical age data from the Eastern Ghats Belt, India; *Geol. Soc. Am. Bull.* **123** 2031–2049.

Bose S, Fukuoka M, Sengupta P and Dasgupta S 2000 Evolution of high Mg–Al granulites from Sunkarametta, Eastern Ghats, India: Evidence for a lower crustal heating–cooling trajectory; *J. Metamorph. Geol.* **18** 223–240.

Butler R W H and Freeman S 1996 Can crustal extension can be distinguished from thrusting in the internal parts of mountain belts? A case history of the Entrelor shear zone, Western Alps; *J. Struct. Geol.* **18** 909–923.

Cawood P A, Kröner A, Collins W J, Kusky T M, Mooney W D and Windley B F 2009 Accretionary orogens through Earth history; *Geol. Soc. London Spec. Publ.* **318** 1–36.

Chetty T R K 2001 The Eastern Ghats Mobile Belt, India: A collage of juxtaposed terranes (?); *Gondwana Res.* **4** 319–328.

Chetty T R K, Vijaya P, Narayana B L and Giridhar G V 2003 Structure of the Nagavalli shear zone, Eastern Ghats Mobile Belt, India. Correlation in the East Gondowana reconstruction; *Gondwana Res.* **6** 215–229.

Das K, Bose S, Karmakar S and Chakraborty S 2012 Petrotectonic framework of granulites from northern part of Chilka Lake area, Eastern Ghats Belt, India: Compressional vis-à-vis transpresional tectonics; *J. Earth Syst. Sci.* **121** 1–17.

Das K, Bose S, Karmakar S, Dunkley D J and Dasgupta S 2011 Multiple tectonometamorphic imprints in the lower crust. First evidence of ca 950 Ma (zircon U–Pb SHRIMP) compressional reworking of UHT aluminous granulites from the Eastern Ghats Belt, India; *Geol. J.* **46** 217–239.

Das K, Naotaka T, Bose S and Ando J 2013 On oriented ilmenite needles in garnet porphyroblasts from deep crustal granulites: Implications for fluid evolution and cooling history; *Lithos* **156–159** 230–240.

Das S, Nasipuri P, Bhattacharya A and Swaminathan S 2008 The thrust-related contact between the Eastern Ghats Belt and the adjoining Bastar Craton (Eastern India): Evidence from mafic granulites and tectonic implications; *Precamb. Res.* **162** 70–85.

Dasgupta S, Bose S and Das K 2013 Tectonic evolution of the Eastern Ghats Belt, India; *Precamb. Res.* **227** 247–258.

Dasgupta S, Sanyal S, Sengupta P and Fukuoka M 1994 Petrology of granulites from Anakapalle – evidence for Proterozoic decompression in the Eastern Ghats, India; *J. Petrol.* **35** 433–459.

Dasgupta S and Sengupta P 2003 Indo-Antarctic correlation: A perspective from the Eastern Ghats Belt; In: Proterozoic East Gondowana: Supercontinent assembly and breakup (eds) Yoshida M, Windley B F and Dasgupta S, *Geol. Soc. London Spec. Publ.* **206** 131–143.

Dewey J F, Holdsworth R E and Strachan R A 1998 Transpression and transtension zones; In: Continental transpressional and transtensional tectonics (Eds) Dewey J F, Holdsworth R E and Strachan R A; *Geol. Soc. London Spec. Publ.* **135** 1–14.

Dobmeier C 2006 Emplacement of proterozoic massif-type anorthosite during regional shortening: Evidence from the Bolangir anorthosite complex (Eastern Ghats Province, India); *Int. J. Earth Sci.* **95** 543–555.

Dobmeier C J and Raith M M 2003 Crustal architecture and evolution of the Eastern Ghats Belt and adjacent regions of India; In: Proterozoic East Gondowana: Supercontinent Assembly and Breakup (eds) Yoshida M, Windley B F and Dasgupta S, *Geol. Soc. London Spec. Publ.* **206** 145–168.

Dobmeier C and Simmat R 2002 Post Grenvillian transpression in the Chilka Lake area, Eastern Ghats Belt – implications for the geological evolution of peninsular India; *Precamb. Res.* **113** 243–268.

Fossen H 2010 *Structural Geology* (First edn); Cambridge University Press.

Fossen H, Tikoff B and Teyssier C 1994 Strain modelling of transpressional and transtensional deformation; *Nor. Geol. Tidsskr.* **74** 134–145.

Frost B R, Barnes C G, Collins W J, Arculus R J, Ellis D J and Frost C D 2001 A geochemical classification for granitic rocks; *J. Petrol.* **42** 2033–2048.

Middlemost E A K Naming materials in the magma/igneous rock system; *Earth Sci. Rev.* **37** 215–224.

Ghosh S K 1993 *Structural Geology – Fundamentals and Modern Developments*; Pergamon Press Ltd.

Goscombe B D, Hand M, Gray D and Mawby J 2003 The metamorphic architecture of a transpressional orogen: The Kaoko Belt, Namibia; *J. Petrol.* **44** 676–711.

Gupta S 2012 Strain localization, granulite formation and geodynamic setting of 'hot orogens': A case study from the eastern Ghats Province, India; *Geol. J.* **47** 334–351.

Gupta S, Nanda J, Mukherjee S K and Santra M 2005 Alkaline magmatism versus collisional tectonics in the Eastern Ghats Belt, India; *Gondwana Res.* **8** 403–419.

Hippertt J, Rocha A, Lana C, Egydio-Silva M and Takeshita T 2001 Quartz plastic segregation and ribbon development in high grade striped gneiss; *J. Struct. Geol.* **23** 67–80.

Karmakar S, Bose S, Das K and Dasgupta S 2009 Proterozoic Eastern Ghats Belt, India – A witness of multiple orogenies and its lineages with ancient supercontinents; *J. Vir. Explorer* **32** paper 3.

Karmakar S and Fukuoka M 1998 Successive metamorphism from a suite of granulite facies rocks from Araku Valley; Implications for the P–T trajectory in the Eastern Ghats; *Geol. Soc. London Spec. Publ.* **44** 201–219.

Karmakar S and Fukuoka M 1992 Genesis of leptynites: Evidence from Araku Valley, Eastern Ghats, India; *Indian Minerals* **46** 247–258.

Kovach V P, Narayana B L, Rao A T, Yoshida M, Rao P R, Rao V D, Kotov A B and Salkinova E B 1997 Sm–Nd isotopic investigations in the central part of the Estern Ghats Granulite Belt; *Int. Field workshop on Proterozoic Geology of Madagascar; Gondwana Res. Group Misc. Publ.* **5(Abs)** 40.

Middlemost E A K 1994 Naming materials in the magma/igneous rock system; *Earth Sci. Rev.* **37** 215–224.

Moresi L, Betts P G, Miller M S and Cayley R A 2014 Dynamics of continental accretion; *Nature* **508** 245–248.

Mukhopadhyay A K and Bhattacharya A 1997 Tectonothermal evolution of the gneiss complex at Salur in the Eastern Ghats Granulite Belt of India; *J. Metamorph. Geol.* **15** 719–734.

Mukhopadhyay D and Basak K 2009 The Eastern Ghats Belt – A polycyclic granulite terrain; *J. Geol. Soc. India* **73** 489–518.

Narayana B L, Rama Rao P, Reddy G L N and Divakara Rao V 1999 Geochemistry and origin of megacrystic granitoid rocks from Eastern Ghats Granulite Belt; *Gondwana Res.* **2** 105–115.

O'oconnor J T 1965 A classification for quartz-rich igneous rocks based on feldspar ratios; In: US Geol. Surv. Prof. Paper B525 USGS 79–84.

Passchier C W and Trouw A J T 2005 *Microtectonics*; Springer, Berlin-Heidelberg-New York.

Platt J P and Behr W M 2011 Grainsize evolution in ductile shear zones: Implications for strain localization and strength of the lithosphere; *J. Struct. Geol.* **33** 537–550.

Plujim B A van der, Mezger K, Cosca M A and Essene E J 1994 Determining the significance of high-grade shear zones by using temperature-time paths, with examples from the Grenvillian orogen; *Geology* **22** 743–746.

Ramsay J G 1967 *Folding and fracturing of rocks*; McGraw Hill.

Ramakrishnan M, Nanda J K and Augustine P F 1998 Geological evolution of the Proterozoic Eastern Ghats Mobile Belt; *Geol. Surv. India Spec. Publ* **44** 1–21.

Rickers K, Mezger K and Raith M M 2001 Evolution of the continental crust in the Proterozoic Eastern Ghats Belt, India and new constraints for Rodinia reconstruction: Implications from Sm–Nd, Rb–Sr and Pb–Pb isotopes; *Precamb. Res.* **112** 183–210.

Sengupta P, Dasgupta S, Bhattacharya P K, Fukuoka M, Chakraborti S and Bhowmick S 1990 Petrotectonic imprints in the Sapphirine granulites from Anantagiri, Eastern Ghats Mobile Belt, India; *J. Petrol.* **31** 971–976.

Sengupta P, Karmakar S, Dasgupta S and Fukuoka M 1991 Petrology of spinel granulites from Araku, Eastern Ghats, India, and a petrogenetic grid for Sapphirine free rocks in the system FMAS; *J. Metamorph. Geol.* **9** 451–459.

Simmat R and Raith M M 2008 U–Th–Pb monazite geochronometry of the Eastern Ghats Belt, India: Timing and spatial disposition of poly metamorphism; *Precamb. Res.* **162** 16–39.

Streckeisen A 1974 Classification and nomenclature of plutonic rocks; *Geol. Rundsch* **63** 773–786.

Twiss T J and Moores E M 2007 *Structural Geology*, 2nd edn, W.H. Freeman and Company.

Valentin Ez 2000 When shearing is a cause of folding; *Earth Sci. Rev.* **51** 155–172.

Whalen J B, Currie K L and Chappell B W 1987 A type granites: Geochemical characteristics, discrimination and petrogenesis; *Contrib. Mineral. Petrol.* **95** 407–419.